View metadata, citation and similar papers at core.ac.uk
brought to you by CORE
provided by Periodica Polytechnica (Budapest University of Technology and...

PERIODICA POLYTECHNICA SER. TRANSP. ENG. VOL. 47, NO. 1, PP. 167–176 (2004)

SOME STRUCTURAL ASPECTS OF MAGNETIC PROPERTY EVOLUTION IN FINEMET-TYPE SENSOR MATERIAL DURING AMORPHOUS-NANOCRYSTALLINE TRANSFORMATIONS

Ágnes CZIRÁKI*, Olivér UDVARDY**, Antal LOVAS** and Géza TICHY*

*Institute for Solid State Physics
Eötvös University
H–1117 Budapest, Hungary
Tel: +36 1 372 2886; Fax: +36 1 372 2868
e-mail: cziraki@ ludens.elte.hu; tichy@ludens.elte.hu
**Department of Vehicle Manufacturing and Repairing
Budapest University of Technology and Economics
H–1521 Budapest, Hungary
Tel: +36 1 463 1938; Fax: +36 1 463 3467
e-mail: lovas@kgtt.bme.hu; udvardy@kgtt.bme.hu

Received: October 1, 2004

Abstract

Devitrification of glassy $Fe_{73.5}Si_{13.5}B_9Nb_3Cu_1$ alloy used as potential sensor material was followed by magnetic measurements and X-ray diffraction, and transmission electron microscopy. It was found, that the permeability, and the coercive field of the alloy changed well below the crystallisation onset, showing a remarkable increase, which was attributed to the structural relaxation and a heterogen nucleation of iron rich phase on Cu clusters. On the basis of lattice parameter measurements the iron rich clusters were depleted from Si atoms during the nucleation process and the Si atoms built in them only during annealing at higher temperatures as 500 °C and 540 °C forming a DO_3 structure.

From the structural study of samples annealed near to the optimal transformation stage it was concluded, that size distribution of the bcc-Fe(Si) nanocrystallites (not exclusive factor) was only one of the most important factors to achieve the optimal soft magnetic properties, but at the same time, their volume fraction, as well as the degree of ordering in DO_3 structure did also contribute to the property optimization.

The average grain size produced by laser pulse heat treatment was nearly the same, as that obtained during the traditional heat treatments.

Keywords: amorphous-nanocrystalline transformation, sensor material, laser pulse heat treatment.

1. Introduction

Recently, the nanocrystalline $Fe_{73.5}Si_{13.5}B_9Nb_3Cu_1$ alloys can be used as potential soft magnetic elements of magnetic sensors. The superior magnetic properties [1]–[6] are coupled with extreme brittleness when the optimum magnetic properties are reached. Therefore, the lowering of extreme brittleness would be desirable without the significant deterioration of permeability. In this respect the details of the structural knowledge is of high importance. At this optimal stage of phase transformation the $Fe_{73.5}Si_{13.5}B_9Nb_3Cu_1$ alloy consists of very small bcc-Fe(Si) crystallites

with a grain size of about 10nm and a residual amorphous matrix. The crystallites are considerably smaller than the ferromagnetic exchange length, and according to Herzer's model [7, 8] the effective magnetic anisotropy is low, because the crystal anisotropies of many randomly oriented grains are averaged out permitting easy domain wall movement. The random orientation of the nanoscale grains is attributed to reduction in the net magnetocrystalline anisotropy, resulting in high permeability [7, 8]. The small magnetostriction is attributed to the fact, that the annealed nanocrystalline samples consist of an amorphous phase with positive magnetostriction and Fe(Si) phase with negative magnetostriction [9]. At an optimal volume fraction of the formed Fe(Si) phase these two opposite tendencies do compensate each other resulting nearly zero net magnetostriction. Hence, the volume fraction and the structure of the precipitated Fe(Si) phase have a great importance in the property tailoring.

According to the experience, the small amount of alloying elements, as Cu (1 at %), and Nb (3 at %) also have an important role in formation of nanocrystalline bcc–Fe(Si) grains. Cu acts as nucleating element for the bcc-Fe(Si) formation and the addition of Nb atoms hinders their growth according to the EXAFS studies [10, 11]. According to the atom probe analysis the pre-crystallization of Cu clusters can be observed already in very early stages of the process, far below the temperature of nanocrystallization onset [12], stimulating the nucleation of α-Fe grains, in which the local Si concentration is lower in the first period than that for the average Si-content of the precursor alloy [12]. During longer annealing period, the Si atoms gradually build in the bcc α-Fe crystallites, forming ordered DO_3 structure, as Fe_3Si.

In the present work the correlation between the evolution of magnetic properties and the structual feature of nanocrystalline Fe(Si) phase have been investigated, especially at the early stage of phase transformation.

The average grain size was also determined in samples, being subjected to rapid annealings (laser irradiation). The aim was to collect informations about the role of the long-range diffusion in the evolution of the final composition as well as the size distribution of the nanocrystalline Fe(Si) grains.

2. Experimental

Heat treatments were performed in protective (Ar) atmosphere on toroidal cores prepared from Vacuum-schmelze ribbons. The annealing temperature was between 350 °C and 550 °C. The annealing time changed from 10 min to 3 hours.

Permeability is determined using WKPMA 326 type of precision magnetic analyser at 50 Hz. Subsequently 1% mechanical deformation was applied on the heat-treated cores after each annealing to determine the stress-induced permeability changes (stress sensitivity).

Structural evolution of the phase transformation was followed by transmission electron microscopy (TEM) and X-ray diffraction (XRD). For TEM investigations a Philips M20 microscope was used, and the ribbons were thinned electrochemically

in a solution of perchloric acid and ethanol with a ratio of 1:7 at – 40°C.

The structure of samples (annealed to various degrees of crystallisation) was analysed by a Philips X' Pert type X-ray diffractometer. The resulting Bragg peaks were fitted using the commercial ProFit software. The grain size was determined from the half width of peaks with the help of the Williamson-Hall plot, and the lattice parameters were deduced from each of the measured reflections of bcc Fe, and extrapolated to the 90° Bragg angle.

The laser pulse heat treatments were carried out on 10 mm wide and 26 μm thick FINEMET ribbons using CO_2 laser equipment. The diameter of the treated area was 8 mm, the output power of the laser varied in the range of 50 and 225 W in 25 W steps. The duration of the treatment was 0.5 sec. A special sample holder was constructed for the rapid laser annealing in order to ensure the sufficient heat contact during the laser treatments.

3. Results and Discussion

3.1. Change of Permeability as a Function of Annealing Temperature

Fig. 1 shows the permeability measured at 50 Hz on the $Fe_{73.5}Si_{13.5}B_9Nb_3Cu_1$ alloy annealed at various temperatures for 1 hour. A remarkable increase of permeability was observed already well below the crystallization temperature between 420 °C and 470 °C. A remarkable increase in permeability was detected already in the temperature range of 440 °C–480 °C, which is below the crystallization. This permeability increase can be attributed to the structural relaxation as well as to the heterogen nucleation of α-Fe nanocrystallites with lower Si-content than the average concentration in the alloy. DO_3 ordered phase is formed in the sample, due to annealing around the optimal temperature causing further increase in permeability. The relative permeability change due to 1% deformation exhibits a maximum below the crystallization temperature at 460 °C showing that the stress-sensitivity of the precipitated α-Fe is higher than in the ordered Fe(Si) phase. These observations are in qualitative agreement with the results of earlier coercivity measurements [2] which show that after a first magnetic softening a relative hardening takes place between 400 °C and 450 °C before the final softening can be observed in the sample annealed at 540 °C. The relative permeability change at 50 Hz due to 1% deformation exhibits an abrupt increase achieving a maximum within this temperature range (see *Fig. 2*).

The first magnetic softening around 350 °C can be attributed [2] to a relaxation process, which is coupled with a 'pre-crystalline stage' (from 350° C to 470 °C). The samples exhibit further permeability increase, which can not be interpreted solely by supposing a simple structural relaxation process alone. This is the consequence of nanocrystallization.

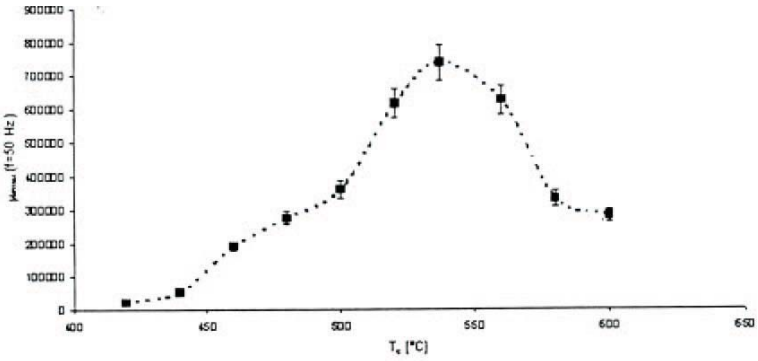

Fig. 1. The permeability measured at 50 Hz on the samples annealed at different temperatures for 1 hour

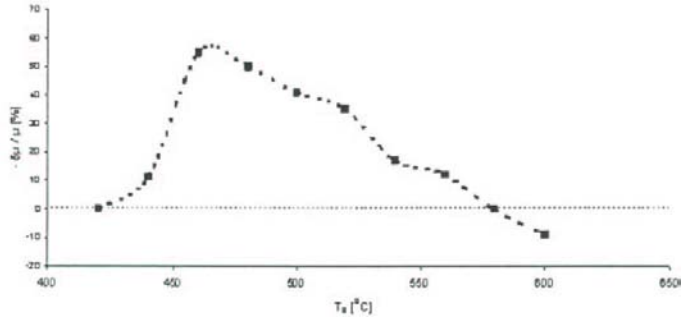

Fig. 2. The relative permeability change at 50 Hz due to 1% deformation versus the temperature of heat treatment for 1 hour

3.2. Structural Manifestation of Relaxation and Clustering Processes below 500 °C

After annealing at low temperatures such as 350 °C or 440 °C for 1 hour, the samples exhibit only a wide amorphous reflection on their XRD patterns. Comparing the as-quenched and the annealed samples a remarkable shift in the position of the amorphous halo towards the larger angles is observed. *Fig. 3* shows the displacement in the angular position of the principal diffraction maximum belonging to the amorphous phase with annealing temperature.

The shift towards higher angles is consistent with a decrease in the average nearest neighbour distance in the amorphous matrix annealed at low temperature (350 °C or 440 °C for 1 h). The shift is nearly the same for both samples annealed at 350 °C or 440 °C.

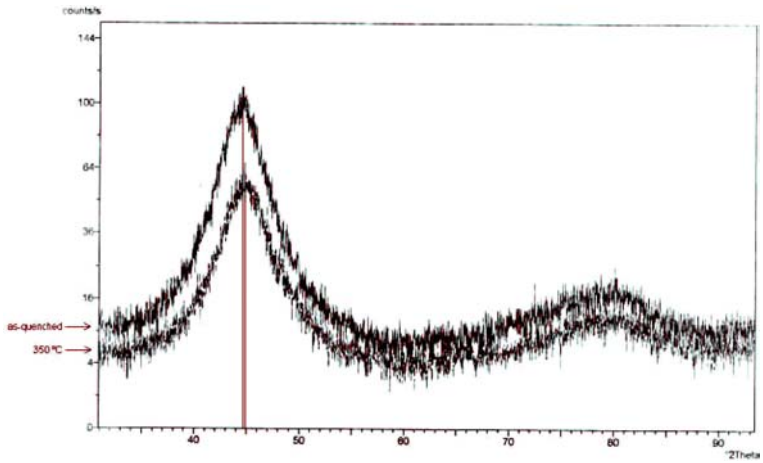

Fig. 3. X-ray diffraction pattern of $Fe_{73.5}Si_{13.5}B_9Nb_3Cu_1$ alloy a) as quenched, and b) annealed at $T = 350$ °C for 1 hour

The same displacement of the diffuse ring was also observed on the electron diffraction patterns (see the SAD patterns shown in *Fig. 4*).

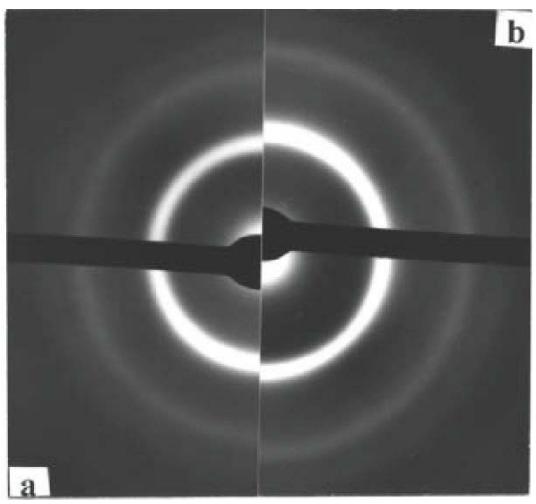

Fig. 4. SAD pattern of $Fe_{73.5}Si_{13.5}B_9Nb_3Cu_1$ alloy a) as quenched and b) annealed at T = 440 °C for 1 hour

The larger part of this increase observed in density of annealed amorphous phase can be ascribed to the structural relaxation taking place prior to the nanocrys-

talline grain formation. On the other hand, it is known from the EXAFS studies [11], that Cu clusters with 'nearly-fcc structure' are present from very early stages of the crystallization process, so the minor part may arise from the formation of dense, 'fcc-like' Cu-rich clusters during the very early stage of crystallization.

The larger part of this shift is the consequence of the well-known density increase associated with the structural relaxation taking place within this temperature range.

In the specimen annealed for 5 min at 400 °C, inhomogeneous distribution of the Cu atoms does appear according to the atom probe analysis, indicating that some clustering of Cu atoms has already started at this temperature even within this very short annealing period [12]. After 60 min annealing at 400 °C this clustering is more clearly visible (sizes are around 3 nm already). One can conclude from these observations, that the Cu-clustering itself can also give some contribution to the net decrease of the nearest neighbour distances, as it is indicated by the amorphous halo shift in the diffraction patterns.

As the HREM image does not give fringe contrast corresponding to any crystalline structure, the structure of Cu clusters formed in the early stage of nucleation was claimed to be unknown [12]. Raising the temperature to 450 °C during 5 min isothermal annealing, primary bcc-Fe nanocrystals ($\sim$7 nm) were already recognized in the high resolution picture [12], whereas no trace of crystalline diffraction ring or spots could be detected in their SAD pattern. The atom probe analysis revealed, that the Cu precipitates were located in contact with bcc-Fe grains, indicating their heterogen nucleation [12]. The α-Fe particles (being nucleated heterogeneously on the Cu cluster) are slightly depleted from Si atoms, i.e. their Si-content is lower, than that for the precursor alloy.

Considering the cited results the X-ray diffraction patterns obtained on samples, being previously annealed at 350 °C or 440 °C for 1 hour, were deconvoluted into a wide amorphous and a Bragg peak, which would be the strongest line for bcc and also for fcc crystal structure (see for example *Fig. 5*).

From the place of the deconvoluted crystalline peak the lattice distance was determined as $d = 0.2029$ nm. This value is slightly higher, than $d_{(110)} = 0.20268$ nm for pure bcc-Fe, and lower than $d_{(111)} = 0.208$ nm for pure fcc Cu phase. This result indicates, that these clusters are really depleted from Si atoms, and their Cu content cannot be excluded.

On the basis of the ratio of integrated intensities, the volume fraction of clusters is approximately 6% after annealings at 350 °C or 440 °C for 1 hour respectively.

The cluster-sizes (counted from the half-with of the deconvoluted crystalline peak) are 7.3 nm and 7.7 nm respectively, which are in agreement with the earlier results obtained from other types of measurements [12].

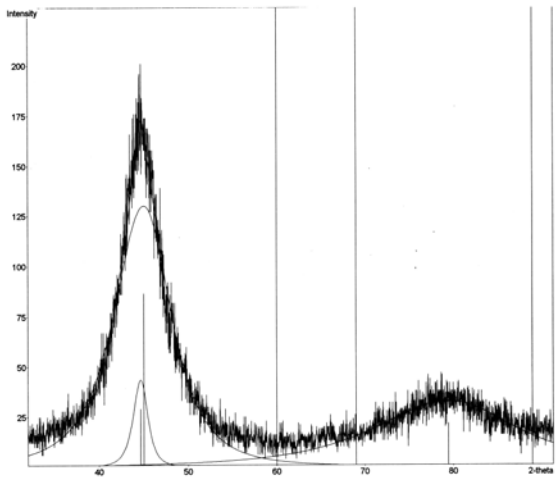

Fig. 5. X-ray diffraction pattern of $Fe_{73.5}Si_{13.5}B_9Nb_3Cu_1$ alloy annealed at $T = 440\,^{\circ}C$ for 1 hour, which was deconvoluted into the amorphous and a Bragg peak of crystalline clusters

3.3. The Evolution of Ordered bcc Fe_3Si phase

TEM picture and the corresponding selected area electron diffraction pattern (SAD) obtained from the sample annealed at 500 °C for 1 hour show, that bcc-Fe phase precipitates from amorphous matrix with an average grain size of about 10 nm (*Fig. 6a*).

Fig. 6b shows, that weak superreflections of the ordered DO_3 structure appear inside the most intensive (110) reflection (see the brightest ring) of the bcc-Fe phase.

On the XRD pattern taken on the same sample the superreflections are also visible. Their origin is the ordering of Si atoms inside bcc-Fe crystallites. The average grain size does not increase with rising temperature, until 540°C (heat treatment condition for achieving superior magnetic properties, especially low magnetic loss at high frequencies). As the annealing temperature rises the grain size does not increase until 540 °C which is considered as the optimum for the nanocrystallization in this alloy. Comparing the TEM pictures taken on the samples annealed at 540°C or 500 °C for 1 hour respectively, one can see, that the average crystalline size is the same (*Fig. 7* and *Fig. 6a*) This result is also confirmed by the XRD measurements. The average crystalline sizes (determined from the half-with of XRD peaks) are 9.6 nm and 9.8 nm.

After the peak deconvolution performed by commercial Pro Fit software, the volume fraction of the crystalline phase was determined from the ratio of integrated intensities of the amorphous and crystalline peaks. In the sample annealed at the

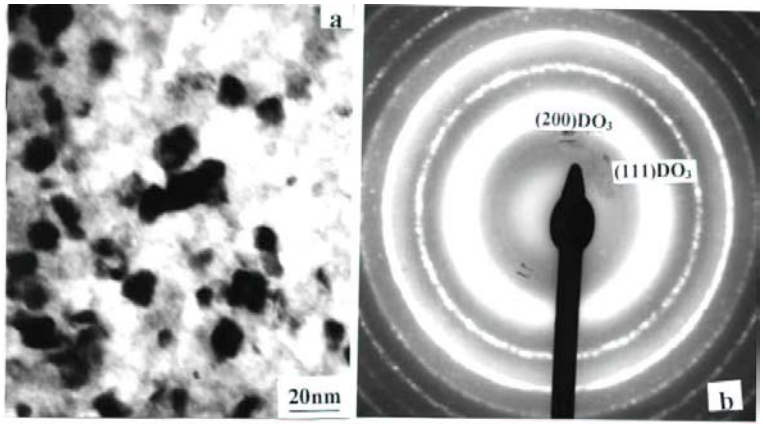

Fig. 6. Bright field TEM picture taken on the $Fe_{73.5}Si_{13.5}B_9Nb_3Cu_1$ sample annealed at T = 500 °C for 1 hour a), and the inner part of the corresponding SAD pattern, where the weak rings correspond to the (111) and the (200) superreflections of the DO_3 ordered FeSi phase b)

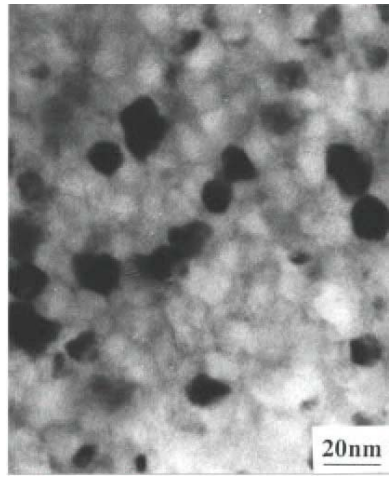

Fig. 7. Bright field TEM picture taken on the $Fe_{73.5}Si_{13.5}B_9Nb_3Cu_1$ sample annealed at 540 °C for 1 hour

early stage of crystallization process (at 500 °C) the volume fraction of the bcc crystalline Fe(Si) phase is around 30%, while under heat treatment conditions near to the optimum (540 °C, 1h) it is approximately 70%.

The XRD patterns of the sample annealed at various temperatures exhibit

differences in the position of the bcc-Bragg peaks and also in the intensity of the superreflections, what becomes gradually stronger as the temperature of heat treatment is increasing. The displacement of peak positions with annealing temperature was analysed. The systematic shift towards the larger angles with increasing temperature indicates that the lattice parameter of the bcc phase gradually decreases, due to the increasing Si-content of the bcc-Fe phase.

Both the decrease of the lattice parameter and the intensity increase of the superreflctions suggest, that Si atoms diffuse most intensively into the bcc-Fe crystallites at around 540 °C, rather than at lower temperature raising the Si-content and simultaneously completing the ordering.

Our results including the appearance of superreflections at the early stage of the crystallization process (at 500 °C), are in good agreement with the earlier observations [11] which established, that the ordered character of the bcc-Fe crystallites appears already in the early stage of decomposition.

It was found, that the average grain size is higher in the laser irradiated samples, than that in the conventionally heat-treated ones. Si-content is also higher in the laser irradiated samples. This result does also confirm the rapid Si diffusion into the α-Fe nanograins at temperatures around 540 °C. This means that in the case of adequately high temperature the final Si-content of the nanocrystallites sets in after a short time.

4. Conclusions

It is confirmed by the presented results, that iron-rich grains are nucleated on the Cu-clusters during the first step of the amorphous-nanocrystalline transformation of FINEMET type precursors. The findings do support the eutectoidal nature of the nucleating events in this type of alloys, proposed by [14, 15]. The volume fraction of this Fe-rich crystallites is approximately 6% in the samples annealed in the temperature range of 350 °C–440 °C for 1 hour. Their estimated sizes are about 7.3 nm and 7.6 nm respectively.

The lattice parameter of bcc crystallites is larger in the early stage of crystallization than that for the pure α-Fe, which hints to the 0.2866 nm lattice parameter of pure α-Fe; it could be concluded, that they are depleted from Si, whereas they could contain Cu atoms.

The detected increasing value of permeability and the relative magnetic hardening [2] are attributed to the formation of nearly pure fine Fe crystallites below crystallization temperature which could be determined by calorimetric measurements.

In agreement with [13] DO_3 gradually ordered structure precipitates already in the early stage of crystallization by applying isothermal heat treatments.

Comparing the microstructures of the samples formed just at the beginning (500 °C) and the final stage of nanocrystallization (540 °C) it was established, that the size of the bcc-Fe(Si) nanocrystallites is not solely responsible for the

development of excellent soft magnetic properties. The volume fraction and the ordering do also contribute to property evolution taylored for a given purpose.

Acknowledgements

This work has been supported by the Hugarian Scientific Research Fund (OTKA) through grants No. T-035278 and T-046239.

References

[1] YOSHIZAWA, Y. – OGUMA, S. – YAMAUCHI, K., *Journal of Appl. Phys*, **64** No. 10 (1988) pp. 6044.
[2] MOYA, J. – VÁZQUEZ, M. – CREMASCHI, V. – ACONDO, B. – SIRKIN, H. *Nano Structured Mat.*, **8** No. 5 (1997), pp. 611–621.
[3] YAVARI, A. R. – NEGRI, D., *Nano Structured Mat.*, **8** No. 8 (1997), pp. 969–986.
[4] CHEN, W. Z. – RYDER, P. L. *Mat. Scie and Engineering*, **B 34** (1995), pp. 204–209.
[5] ZHANG, X. Y. – ZHANG, J. W. – XIAO, F. R. – LIU, J. H. – LIU, R. P. – ZHAO, J. H. – ZHENG, Y. Z. *Materials Letters*, **34** (1998), pp. 85–89.
[6] CHEN, W. Z. – RYDER, P. L., *Mat. Sci. and Engineering*, **B 49** (1997), pp. 14–17.
[7] HERZER, G., *IEEE Trans. Magn.*, **25** No. 5 (1989), p. 3327.
[8] HERZER, G., *IEEE Trans. Magn.*, **26** No. 5 (1990), p. 1397.
[9] HERZER, G., *Mat. Scie and Engineering*, **AI 33** (1991), pp. 1–5.
[10] MÜLLER, M. – MATTERN, N. – ILLGEN, L., *J. Magnetism and Magnetic Materials*, **112** (1992), p. 263.
[11] AYERS, J. D. – HARRIS, V. G. – SPRAGUE, J. A. – ELAM, W. T. – JONES, H. N., *Acta Mater.*, **46** No. 6 (1998), pp. 1861–1874.
[12] HONO, K. – PING, D. H. – OHNUMA, M. – ONODERA, H., *Acta Mater.*, **47** No 3 (1999), pp. 997–1006.
[13] CZIRÁKI, Á. – GERÖCS, I. – VARGA, L. K. – BAKONYI, I. – FALKE, U. – BAUER, H. D. – WETZIG, K., *Z. Melallkd.*, **93** (2002), p. 1.
[14] LOVAS, A. – VÁZQUEZ, M., *Acta Electronica et Informatica*, **3** No. 2 (2002), p. 86.
[15] JUHÁSZ, R. – CZIRÁKI, Á. – KISS, L. F. – LOVAS, A., *Materials Science and Engineering*, **A 375–377** (2004), pp. 1057–1061.